

*Chapter 2*

**EXPERIMENTAL DETAILS**



## 2. Experimental details

### 2.1. Procurement of chemicals and materials

Various chemicals of analytical grade used in the present investigations were: nitric acid, sulfuric acid, hydrochloric acid (Molychem India Pvt. Ltd, India & Fisher Scientific, UK); sodium chloride, sodium bromide (GS Chemical testing lab & Allied industries, India); kerosene (Sigma-Aldrich); toluene (Sisco Research Laboratories Pvt. Ltd, India); bisphenol-A (Otto Chemie Pvt. Ltd, India); acetone and ethanol (Fisher Scientific, India); Dimethylacetamide (Central Drug House (P) Ltd., India); ammonia solution (Loba Chemie Pvt. Ltd., India); ACORGA M5640 (Cytec India speciality chemicals & materials Pvt. Ltd., India) and distilled water. Organic amides such as primary ( $1^\circ$ ,  $L^1$ ), secondary ( $2^\circ$ ,  $L^2$ ) and tertiary ( $3^\circ$ ,  $L^3$ ) amides were synthesized in the laboratory of school of chemistry, The University of Edinburgh according to literature methods and used. Obsolete mobile phones used in this work (Nokia, Samsung GSM) were collected from the local e-scrap vendors in Varanasi, India.

### 2.2. Pre-processing of WPCBs

WPCBs were initially separated from mobile phones by manual dismantling from the other major components such as batteries, keyboard and screen monitor glass. The detachment of electronic components such as resistors, capacitors, ICs, transistors, and diodes was executed by mild heating the soldered joints with a *Stanley STXH 2000-IN* heat gun ( $T < 200^\circ\text{C}$ ) and a plier. Bare PCBs were then separated and cleaned with hot water followed by acetone to remove any grease, dirt and other contaminants. Detached components and solder metal were collected and stored in a vacuum desiccator separately. All cleaned WPCBs were cut manually into squares ( $1 \times 1 \text{ cm}^2$ ) using a shear cutter. Downsized PCBs were cleaned again with hot distilled water to remove further

adhesive matter, dried for 24 h at 30 °C and stored in a desiccator. These cleaned PCB squares were initially pulverized to <math>-1\text{ mm}</math> size using a hammer mill make *Ikon Instruments*, India. The inlet chute at the top of the mill used for the feed and powder was collected from the bottom part of the mill. The maintained feed rate was 3 kg/h. In another step, chopped square PCBs were utilized to separate metallic and non-metallic interwoven laminated layers through chemical pre-treatment. The process used for the delamination of layers, chemical analysis of powder and liberated layers will be explained in the coming subsections in detail. A graphical representation of the pre-processing is shown in **Figure 2.1**.

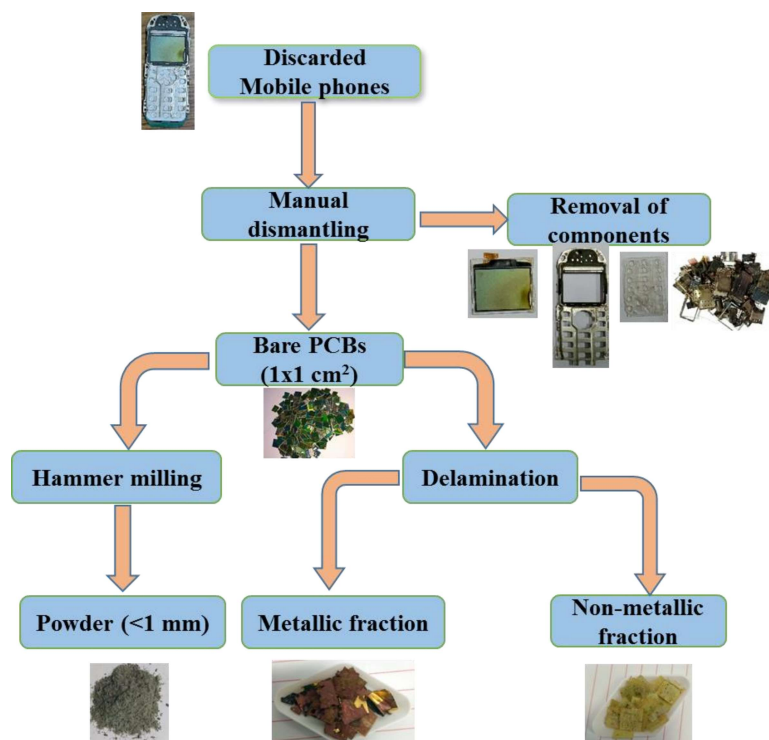


Figure 2.1- Graphical representation of pre- processing of WPCBs

### 2.2.1. Estimation of composition in WPCBs

The composition of the PCB powder was initially determined by Scanning Electron Microscopy (SEM) make *Zeiss Evo-18 Research 2045*, with Energy Dispersive X-ray Spectroscopy (EDS) attachment make *Oxford X-act INCA x-act*. It indicates that the

distribution of metallic and non-metallic fraction is not uniform and showed varying composition as shown in **Figure 2.2**. Non-metallic glass fraction possesses a bamboo-like shape consisting silicon, oxygen and aluminium as major elements along with some attached minor precious elements such as gold and palladium (spectrum 3). Similarly, an examination at metallic fraction illustrates the presence of copper, gold, silver, tin and palladium attached to the glass fiber (spectrum 2).

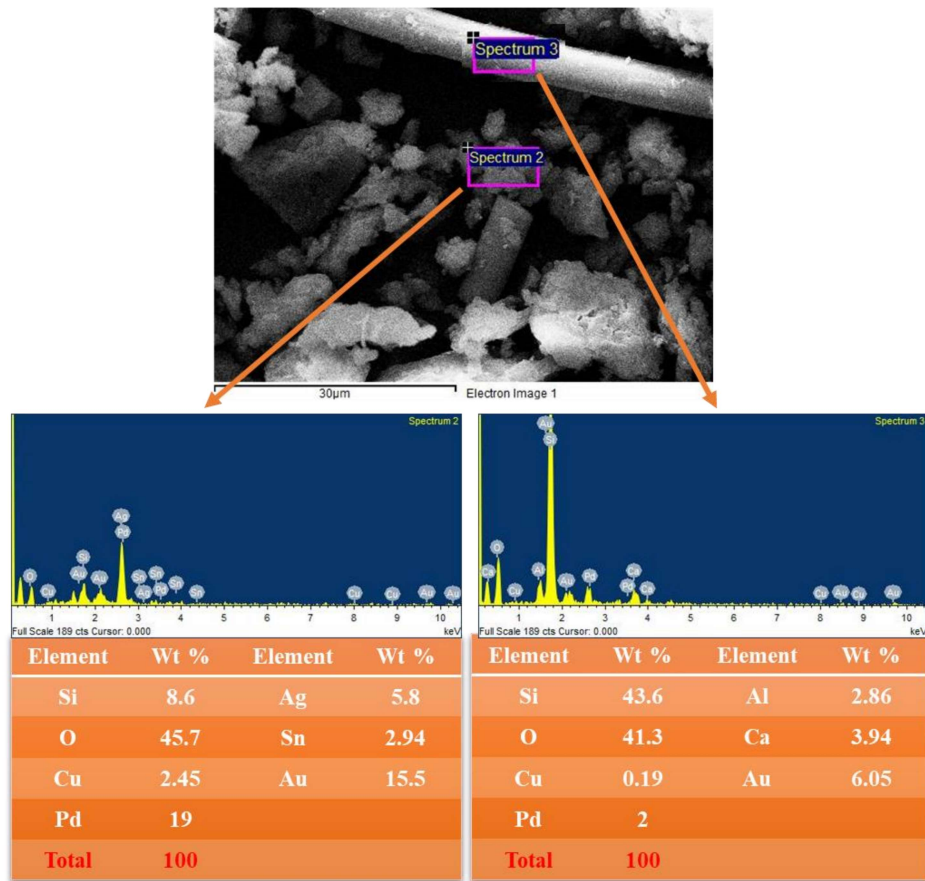


Figure 2.2- SEM-EDS of pulverized WPCBs

The accurate metal composition of the ground WPCBs was also determined using Inductively Coupled Plasma-Optical Emission Spectroscopy (ICP-OES) make *Optima 8300*. For this, 2 g of powder was dissolved in freshly prepared aqua regia for the digestion of metallic values. Initially, aqua regia was poured into a three-necked round

bottom flask and heated using a hot plate with magnetic stirrer setup with a PID controller and thermocouple arrangement. Once pre-set temperature is attained, the powder sample was slowly added into the reaction vessel for the digestion. A condenser was fitted on the central neck to condense any vapours escaping from the system. Continuous agitation was provided by a PTFE coated magnetic stirrer bar. Once the whole metallic portion dissolved in aqua regia, the undissolved non-metallic fraction was separated by filtration using filter paper (Whatman no. 42). Filtered liquor was diluted to a known volume by the addition of distilled water. A small portion of the sample was collected from the solution and diluted with distilled water according to the working range of each element of ICP-OES. Analysis indicates that the PCB powder comprises 42.7 wt% copper and 0.0013 wt% gold, along with other metals (2.4 wt%), plastics and ceramics (54.8 wt%) as shown in **Table 2.1**. Based on this, the milled powder had a relatively lower metallic fraction for leaching operation. At the same time, PCBs also inhibit the leaching recovery rate due to their structure consisting lamination of interwoven layers of metal clad and non-metallic substrates [165]. Therefore, it is planned to separate the layers by dissolving epoxy resin which acts as a reinforcing agent, in an organic solvent.

Table 2.1- Composition of obsolete mobile phone PCBs

Element	(wt%)	Element	(wt%)
Cu	42.73	Pd	0.003
Au	0.0013	Ni	0.4
Ag	0.08	Zn	0.23
Sn	1.33	Pb	0.08
Fe	0.32	Cd	0.1
Plastic and ceramic residues			54.73

### 2.2.2. Chemical pre-treatment: Delamination of layers by dissolving resin in an organic solvent

Downsized square PCBs (1x1 cm<sup>2</sup>) were used for the chemical pre-treatment processing i.e. delamination of metallic and non-metallic layers by dissolving the attached epoxy resin in N, N-dimethylacetamide (DMA) (3:10 solid to liquid ratio) at 160 °C [166]. *REMI IRML, India* heat mantle setup with 1 litre round bottom three-necked mouth flask was used for the dissolution. The gradual dissolution of epoxy resin into DMA was monitored by UV-visible spectrophotometry make *Agilent Cary 60*. While epoxy resin polymer chain consists of Bisphenol-A (BPA) as a major constituent, the resin concentration was measured against the concentration vs absorbance curve plotted for BPA diluted in ethanol as reported by Verma et al., (2016) [72]. After sufficient resin dissolution, the organic solvent was separated by vacuum filtration, and stored carefully for the effective re-generation. The separated metal clads were washed with distilled water appropriately to eliminate attached organic matter, dried at 80 °C for 12 h. The photographs of the gradual dissolution of resin in organic solvent and the liberation of layers are illustrated in **Figure 2.3** with various points from 1 to 4.

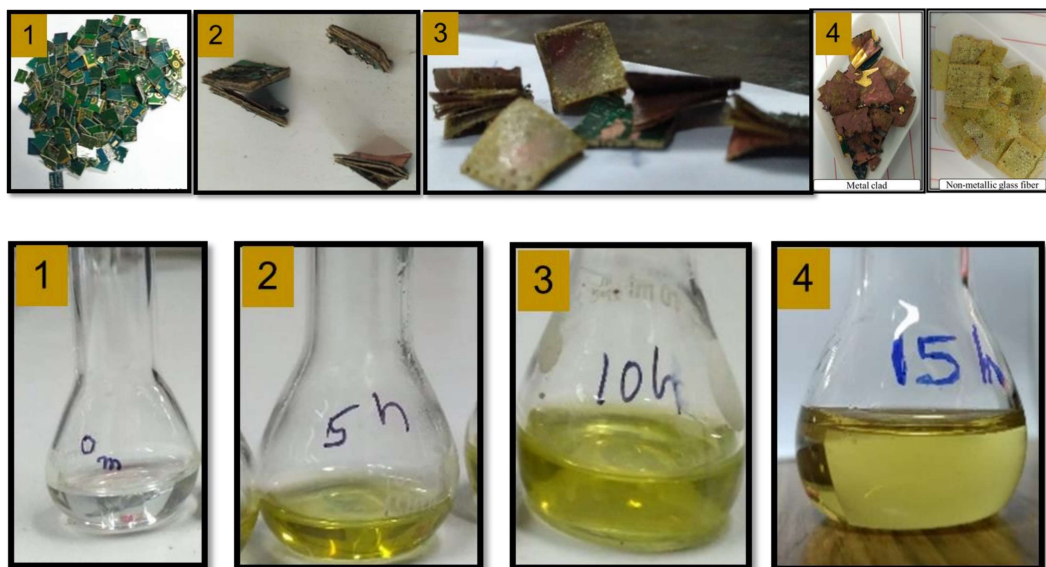
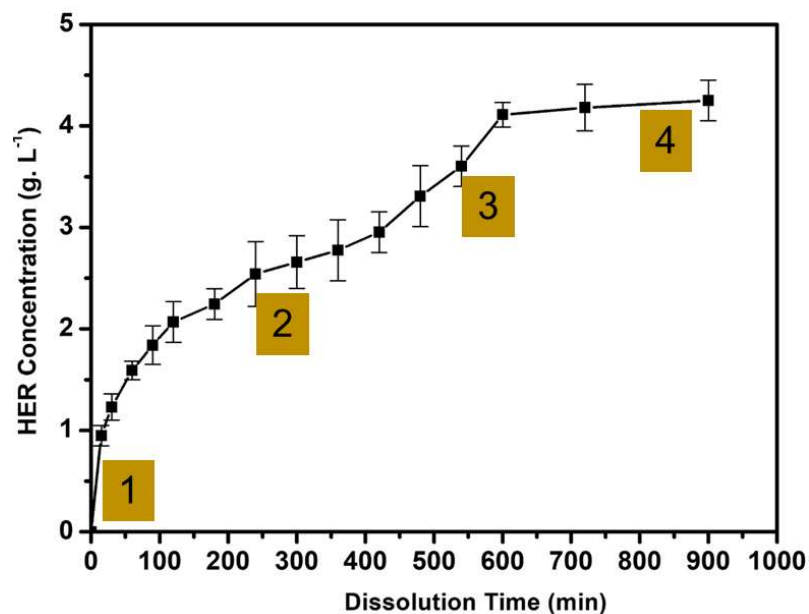


Figure 2.3- Photographs of separation of metallic and non-metallic fraction and dissolution of resin during delamination of WPCBs

### 2.2.3. Analysis of liberated metallic fraction

Metallic fraction obtained from the chemical pre-treatment process was initially analyzed with X-ray diffractometer make Malvern Panalytical Empyrean model with pixel 3D detector using Co-K $\alpha$  ( $\lambda = 1.789 \text{ \AA}$ ) radiation in  $2\theta$  angular range of  $15^\circ$  to  $100^\circ$ , at a

scanning speed of  $0.5^\circ/\text{min}$  with increments of  $0.02^\circ$ . Phases were identified with the help of the ICDD PDF2 database. The XRD pattern indicates the presence copper peaks at around  $50.7^\circ$ ,  $59.3^\circ$  and  $88.8^\circ$   $2\theta$  positions, and other peaks for trace metallic fraction were suppressed by high intense copper peaks (**Figure 2.4**). Similarly, SEM-EDS photographs represent the presence of copper (90 wt%) and other minor elements as displayed in **Figure 2.5**.

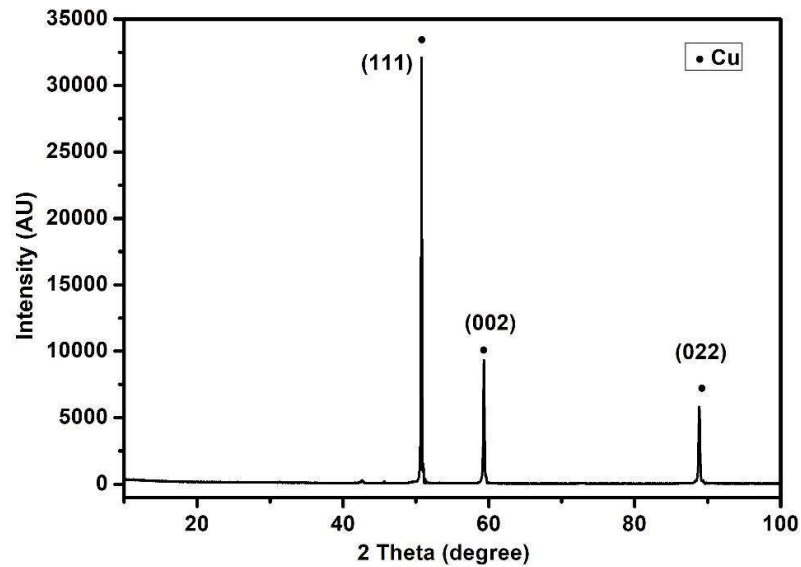


Figure 2.4- XRD analysis of metal clad [167]

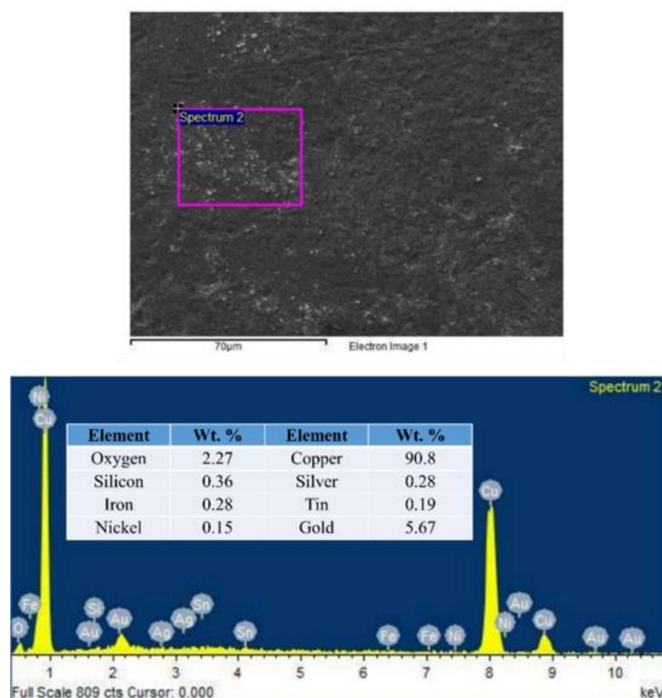


Figure 2.5- SEM-EDS analysis of metal clad

Accurate metal concentrations for the metallic and non-metallic glass fiber layers were obtained by dissolving the metallic values at 50 °C in freshly prepared aqua regia as discussed in **section 2.2.1**. The dissolved portion was filtered, accurately diluted with distilled water and analyzed by ICP-OES. Plastic/ceramic concentrations were inferred. From **Table 2.2**, it was observed that copper occupies a major portion (83.93 wt%) along with other elements in liberated metal clads and the concentration of metallic fraction was also enriched after delamination. So, these layers can be used for the leaching of metals by reducing the overall energy consumption with maximum recovery. Note that after delamination, no iron is seen and the reduction in the quantity of tin is due to the removal of solder attachments before delamination. The delaminated non-metallic fraction (glass fiber) comprises almost all plastics and ceramics (97 wt%) (**Table 2.2**).

Table 2.2- Chemical analysis of delaminated metallic and non-metallic fractions

Element	Delaminated metal fraction (wt%)	Glass fiber after delamination (wt%)
Cu	83.93	2.69
Au	0.046	0
Ag	0.028	0
Sn	0.45	0.04
Fe	0	0
Pd	0.007	0
Ni	2.34	0.36
Zn	0.45	0
Pb	0.1	0
Cd	0.27	0
Plastic and ceramic residues	12.38	97

### 2.3. Two-stage Leaching

The liberated metallic fraction collected from the pre-processing step was leached in two stages. In the first stage, samples were dissolved in dilute nitric acid at various concentrations, which almost exclusively leached copper and nickel by leaving gold in the residue. After complete dissolution, the filtrate was separated, diluted to known volume using distilled water and stored for further purification. The residual gold-rich solids were separated, dried at 80 °C overnight and their chemical composition was determined using SEM-EDS. The accurate metal content was also determined with Atomic Absorption Spectrophotometer (AAS) make *Elico SL 168* by dissolving them in aqua regia as mentioned in **section 2.2.1**. The residue was subjected to a second stage leaching process where sulfuric acid with halide salts (NaCl, NaBr) were used at a variety of concentrations for the selective dissolution of gold and silver. After quantitative

dissolution of gold at optimized parameters, the filtrate was separated, diluted to known volume using distilled water and stored for further purification treatments.

All leaching experiments were conducted in a 100 mL three-necked glass flat-bottom flask. A hotplate with a magnetic stirrer setup containing a PID controller with thermocouple arrangement was used for heating. Silicone oil was used for the transfer of heat to the reaction flask. Each experiment was conducted with a known quantity of liberated metallic sheets (5 g) added to 40 mL of leach solution after heating to a pre-set temperature. Various experiments were conducted to study the effective leaching by changing different parameters such as temperature, time, type of solvent, concentration of solvent, pulp density, and stirring speed. Samples were collected at regular intervals in each experiment, diluted with distilled water, and analyzed by AAS and ICP-OES. Experiments were triplicated and the average readings were noted. The photograph of leaching experiment setup is shown in **Figure 2.6**.

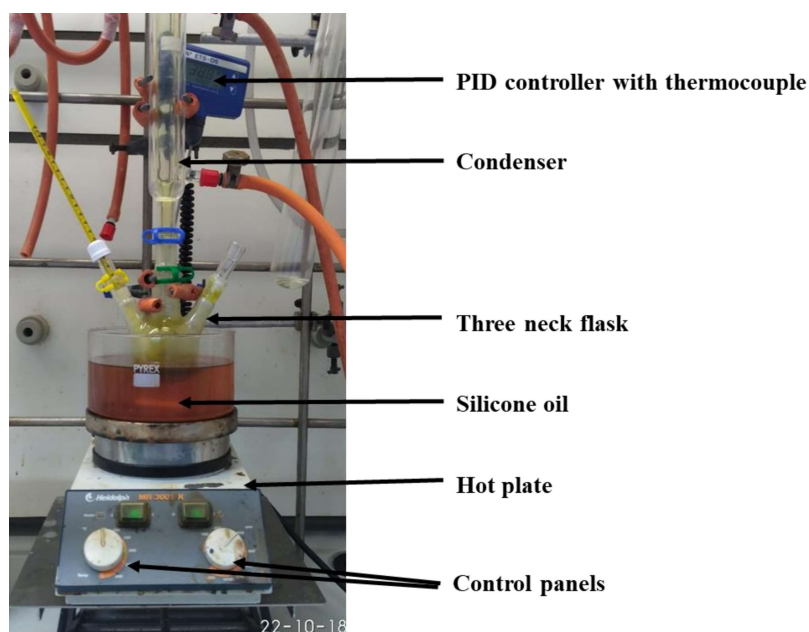


Figure 2.6- Photograph of leaching experiment setup

## 2.4. Solvent extraction

### 2.4.1. Separation of copper and nickel

The acidic leach filtrate collected from stage-1 leaching was adjusted to known pH through the controlled addition of 2 M ammonia solution. The pH of the aqueous solution was measured using a pH-meter make *Labman, LMPH-10*. To allow the selective separation of copper from multi-metal leach solution, the phenolic oxime (under the brand name of ACORGA M5640) dissolved in kerosene (800 g/L) was used as the extractant in stage-1 solvent extraction (SX1). Various parameters were studied for copper extraction including organic to aqueous phase ratio, pH of the initial aqueous solution, the concentration of oxime in kerosene and extraction time as mentioned in **Table 2.3**. Parameters were optimized for the effective recovery of copper at a temperature of 30 °C with a total volume of 20 mL. The copper rich organic solution was physically separated from the remaining acidic aqueous phase (raffinate) using a separating funnel once equilibrium has attained. The resulting raffinate was used in the second stage solvent extraction (SX2) for the selective extraction of nickel. The metal-loaded organic phase was stripped with another aqueous acid at 1:1 organic to aqueous phase ratio at 30 °C for 60 min. Various parameters for the stripping process are also mentioned in **Table 2.3**. The photographs of the copper extraction process are shown in the **Figure 2.7**.

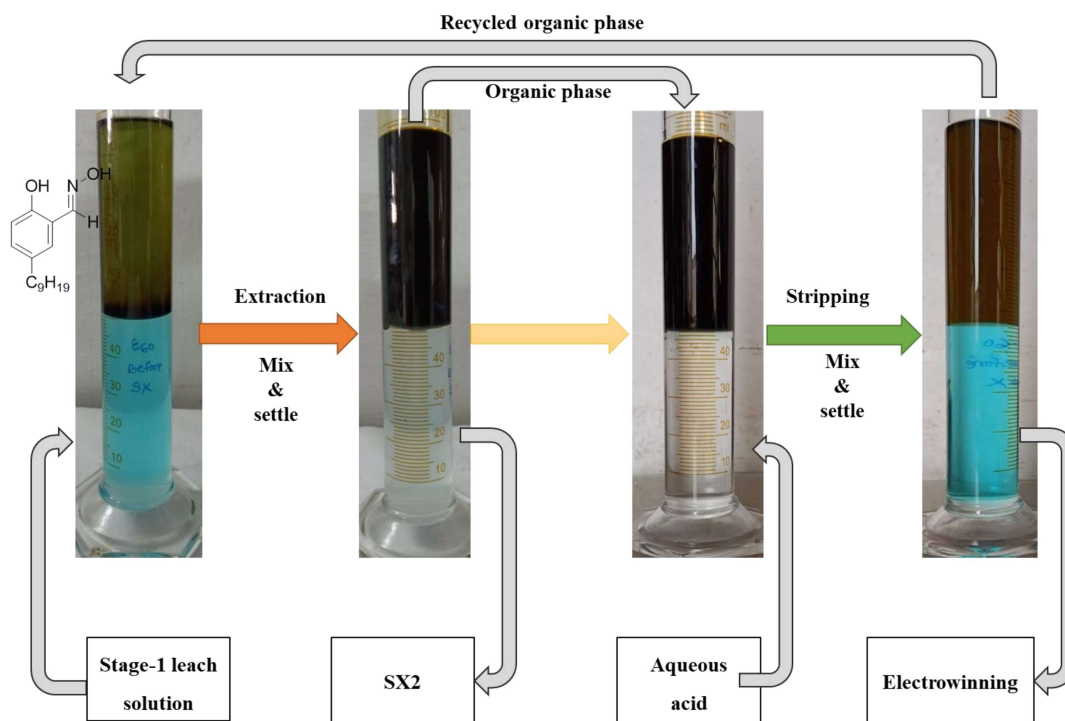


Figure 2.7- Photographs of the process of solvent extraction for copper from stage-1 leach solution

Table 2.3- A summary of the conditions investigated in the recovery of copper in SX1

Unit Operation	Extraction	Stripping
Reagent for extraction or stripping	ACORGA M5640	$H_2SO_4$ and $HNO_3$
Diluent	Kerosene	
Concentration	10-30 vol%	4 M
pH	1-3.5	Depends on stripping agent
Organic : aqueous phase volume ratio	1:2, 1:1.5, 1:1, 1.5:1, 2:1	1:1
Equilibration time	15-60 min	60 min
Temperature	30 °C	30 °C
Stirring speed	600 rpm	600 rpm

For the selective separation of nickel in SX2, ACORGA M5640 was used again as an extractant. Various experiments were conducted over the pH range 3-10 through the controlled addition of 2 M ammonia solution. Other parameters including altering the organic to aqueous phase ratio, the concentration of extractant and agitation time were also optimized for the effective recovery of nickel at a temperature of 30 °C. The aqueous and organic phases were physically separated after equilibrium was reached, and the separated nickel-loaded organic phase was subsequently stripped with HCl, HNO<sub>3</sub> or H<sub>2</sub>SO<sub>4</sub>. The stripping process was carried out at 1:1 organic to aqueous phase ratio at 30 °C for 1 h. The resulting raffinate was used for the removal of traces through further purification processes such as cementation. The different stages of the solvent extraction process for nickel recovery are shown in **Figure 2.8**. The various parameters used for the nickel solvent extraction and stripping are documented in **Table 2.4**.

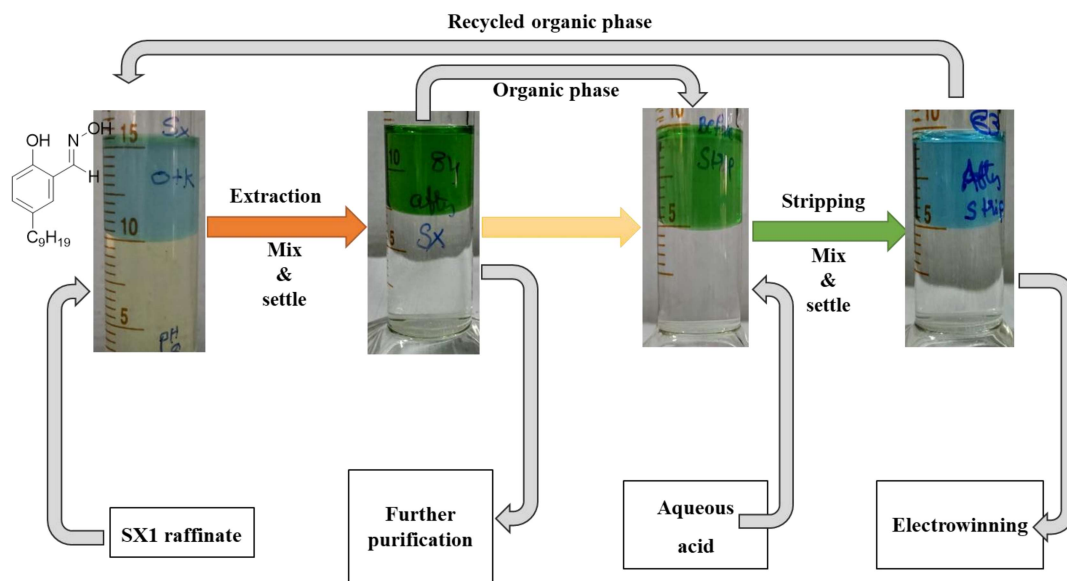


Figure 2.8- Photographs of the process of solvent extraction for nickel

Table 2.4- A summary of the conditions investigated in the recovery of nickel in SX2 [132]

Unit Operation	Extraction	Stripping
<b>Reagent for extraction or stripping</b>	ACORGA M5640	H <sub>2</sub> SO <sub>4</sub> , HNO <sub>3</sub> and HCl
<b>Diluent</b>	Kerosene	Distilled Water
<b>Concentration</b>	1-35 vol%	0.1 – 1 M
<b>pH</b>	3-10	Depends on stripping agent
<b>Organic : aqueous phase volume ratio</b>	1:50, 1:20, 1:10, 1:5, 1:2, 1:1.5, 1:1, 1.5:1, 2:1	1:1
<b>Equilibration time</b>	15-60 min	60 min
<b>Temperature</b>	30 °C	30 °C
<b>Stirring speed</b>	600 rpm	600 rpm

All solvent extraction experiments were carried out in a 30 mL glass measuring cylinder. A PTFE-coated hotplate with magnetic stirrer was used for agitation. After stripping, the used organic solution was separated and used in multiple cycles to check its efficiency. All experiments were performed in triplicate and the samples from each stage were collected and analyzed by AAS.

### 2.4.2. Separation of gold

#### 2.4.2.1. Synthesis of organic amides

All organic amides (Primary (L<sup>1</sup>), secondary (L<sup>2</sup>) and tertiary (L<sup>3</sup>)) were synthesised according to the literature reports [136], [137]. The primary amide was synthesised from its acid chloride and an aqueous ammonia in good yield. The precipitate formed is dissolved in DCM and washed with water to purify and finally producing L<sup>1</sup> as a bright white solid. The L<sup>2</sup> and L<sup>3</sup>, were also synthesised in good yield from the same acid chloride as L<sup>1</sup> and either methylamine or dimethylamine. The products were purified by

a simple extraction into DCM followed by a wash with water, eventually producing the extractants as colourless oils. These amides are sufficiently soluble in toluene for solvent extraction experiments to be carried out. The synthesis of **L<sup>1</sup>**, **L<sup>2</sup>** and **L<sup>3</sup>** are shown in **Figure 2.9**. <sup>1</sup>H-NMR of the amides are also shown in **Figure 2.10** to **Figure 2.12**. All NMR spectra were recorded at 300 K at the school of chemistry, the university of Edinburgh, Scotland, UK. <sup>1</sup>H-NMR was performed on a Bruker AVA500 spectrometer at 500.12 MHz.

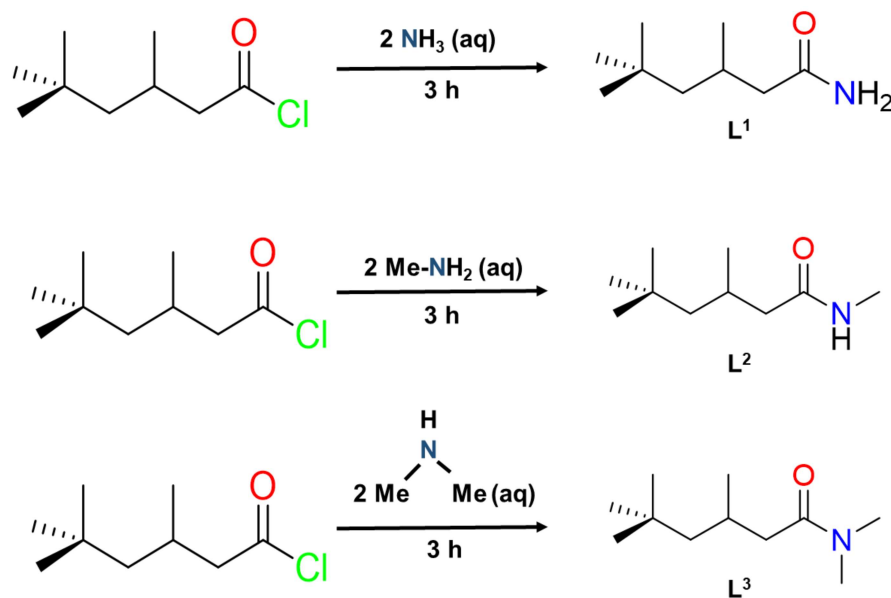


Figure 2.9- Synthesis of Primary (**L<sup>1</sup>**), secondary (**L<sup>2</sup>**) and tertiary (**L<sup>3</sup>**) amides

$^1\text{H-NMR}$  of primary amide:

$^1\text{H NMR}$  (500 MHz,  $\text{CDCl}_3$ )  $\delta$  5.44 (d,  $J = 42.9$  Hz, 2H,  $-\text{NH}_2$ ), 2.26 (dd,  $J = 13.6, 5.4$  Hz, 1H,  $-\text{CH}$ ), 2.01 (dd,  $J = 13.6, 8.5$  Hz, 2H,  $-\text{CH}_2$ ), 1.28 (dd,  $J = 14.0, 3.9$  Hz, 1H,  $-\text{CH}$ ), 1.18 – 1.12 (m, 1H,  $-\text{CH}$ ), 1.03 (dd,  $J = 6.4, 3.0$  Hz, 3H,  $-\text{CH}_3$ ), 0.96 – 0.92 (m, 9H,  $3\text{CH}_3$ ).

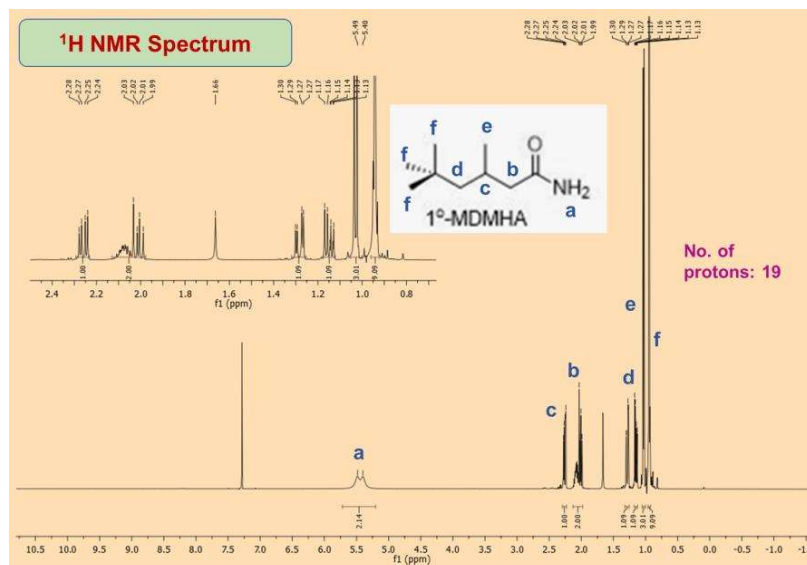
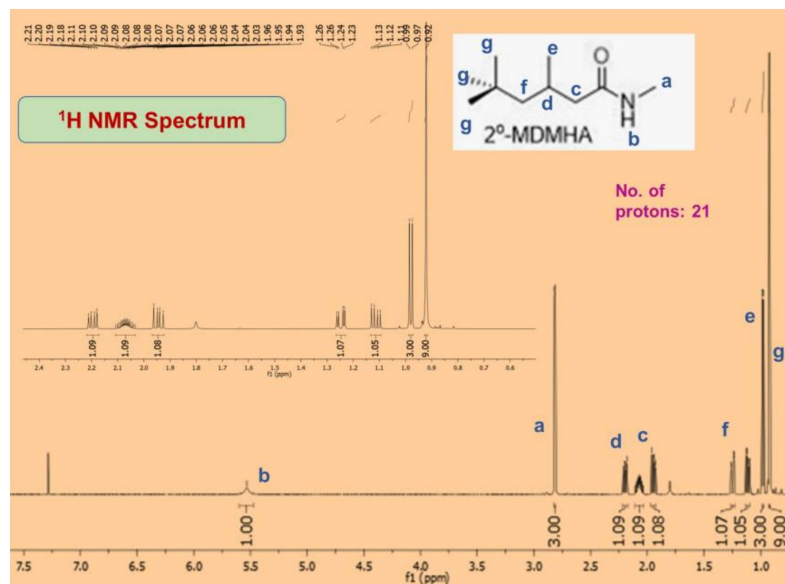


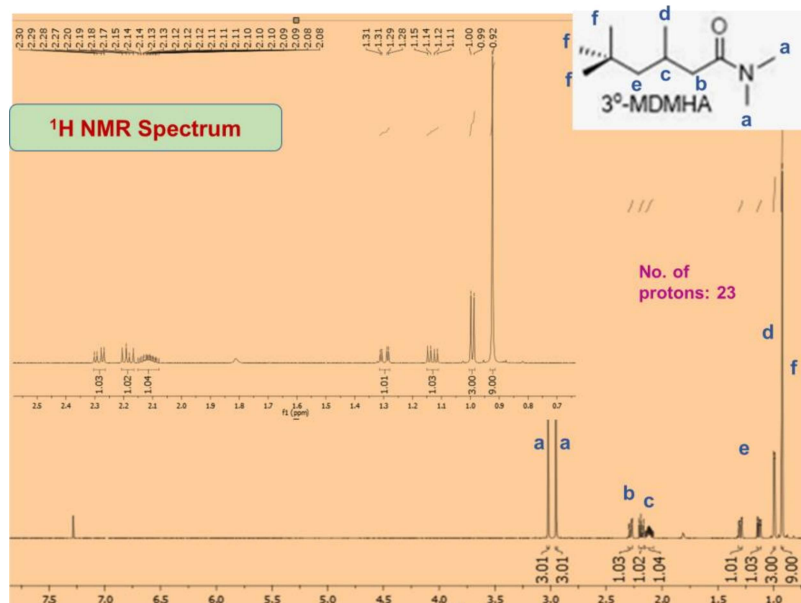
Figure 2.10-  $^1\text{H-NMR}$  of primary ( $1^\circ$ ,  $L^1$ ) amide

 $^1\text{H-NMR}$  of secondary amide:

$^1\text{H-NMR}$  (500 MHz,  $\text{CDCl}_3$ ):  $\delta$  6.32 (s, 1H, NH), 2.74 (d, 3H,  $\text{N}(\text{CH}_3)$ ), 2.15 (dd, 1H,  $\text{CH}_2\text{CO}$ ,  $J = 13.6, 5.9$  Hz), 2.08–1.96 (m, 1H,  $\text{CH}(\text{CH}_3)$ ), 1.92 (dd, 1H,  $\text{CH}_2\text{CO}$ ,  $J = 13.6, 8.3$  Hz), 1.19 (dd, 1H,  $\text{CH}_2\text{C}(\text{CH}_3)_3$ ,  $J = 14.0, 3.9$  Hz), 1.05 (dd, 1H,  $\text{CH}_2\text{C}(\text{CH}_3)_3$ ,  $J = 14.0, 6.6$  Hz), 0.91 (d, 3H,  $\text{CH}(\text{CH}_3)$ ,  $J = 6.6$  Hz), 0.85 (s, 9H,  $\text{C}(\text{CH}_3)_3$ ).

Figure 2.11- <sup>1</sup>H-NMR of secondary (2°, L<sup>2</sup>) amide<sup>1</sup>H-NMR of tertiary amide:

<sup>1</sup>H NMR (500 MHz, CDCl<sub>3</sub>): δ 2.94 (s, 3H, N(CH<sub>3</sub>)), 2.87 (s, 3H, N(CH<sub>3</sub>)), 2.20 (dd, 1H, CH<sub>2</sub>CO, J = 14.6, 5.7 Hz), 2.11 (dd, 1H, CH<sub>2</sub>CO, J = 14.6, 8.2), 2.08–1.99 (m, 1H, CH(CH<sub>3</sub>)), 1.22 (dd, 1H, CH<sub>2</sub>C(CH<sub>3</sub>)<sub>3</sub>, CH<sub>2</sub>C(CH<sub>3</sub>)<sub>3</sub>, J = 14.0, 3.8 Hz), 1.05 (dd, 1H, CH<sub>2</sub>C(CH<sub>3</sub>)<sub>3</sub>, J = 14.0, 6.5 Hz), 0.91 (d, 3H, CH(CH<sub>3</sub>), J = 6.5 Hz), 0.84 (s, 9H, C(CH<sub>3</sub>)<sub>3</sub>).

Figure 2.12- <sup>1</sup>H-NMR of tertiary (3°, L<sup>3</sup>) amide

### 2.4.2.2. Solvent extraction of gold

The collected solution from the stage-2 leaching was used for the separation of gold through solvent extraction process. An organic amide (0.1 M) (L<sup>1</sup>-L<sup>3</sup>) diluted in toluene was used as an extractant. Experiments were conducted with 25 mL of stage-2 leach sample along with 25 mL toluene solution. A magnetic stirrer arrangement is used for agitation. The effect of type of organic amide was optimized to maximize gold recovery. The gold-loaded organic phase was then separated from the aqueous phase and stripped of the metal using either water or sodium hydroxide. The resulting raffinate was used for the separation of silver by cementation. The pure gold solution was separated after stripping and amide with the organic solution used again for extraction. Aqueous and organic samples in each stage were collected and analyzed by AAS or ICP-OES. The various parameters used for the gold solvent extraction and stripping are documented in

#### Table 2.5.

Table 2.5- A summary of the conditions investigated in the recovery of gold from stage-2 leach solution

Unit Operation	Extraction	Stripping
<b>Reagent for extraction or stripping</b>	Organic amide (L1-L3)	Water and NaOH
<b>Diluent</b>	Toluene	
<b>Concentration</b>	0.1 M	0.1 – 1 M for NaOH
<b>Organic : aqueous phase volume ratio</b>	1:1	1:1
<b>Equilibration time</b>	60 min	60 min
<b>Temperature</b>	20 °C	20 °C
<b>Stirring speed</b>	600 rpm	600 rpm

## 2.5. Separation of silver by cementation

To study the separation of silver from the raffinate of gold solvent extraction stage, the cementation process was adopted. As copper is more electronegative (+ 0.34V) than silver (+ 0.8 V), it can displace and precipitate out silver as per the standard electromotive force (emf) series (**Table 2.6**).

Table 2.6- Standard electromotive force (emf) series of selected metals

S.No.	Metal	Standard electrode potential at 25°C, (V)
1	Au	+1.36
2	Ag	+0.80
3	Cu	+0.34
4	H <sub>2</sub>	0.00
5	Sn	-0.14
6	Zn	-0.76
7	Al	-1.60

Therefore, copper powder (325 mesh, BSS) was used as a sacrificial metal for displacing silver. To study the purity of copper powder, it was initially analyzed by X-ray diffractometer make *Rigaku XtaLAB mini* using Cu-K $\alpha$  ( $\lambda = 1.7544 \text{ \AA}$ ) radiation at a scanning speed of 0.5°/min with increments of 0.02°. Phases were identified with the help of the ICDD PDF2 database and shown in **Figure 2.13**. It can be seen that the presence of high intense copper peaks at around 43.4°, 50.5°, 74.2° and 90°, 2-theta positions. A close examination of wt% of elements was also done with SEM-EDS as shown in **Figure 2.14**. It was observed that the purity of copper was approximately 99 wt% along with traces of tin. The surface area of the copper powder (0.505 m<sup>2</sup>g<sup>-1</sup>) was also determined

by BET (Brunauer, Emmett and Teller) surface area analyzer make “*MicrotracBEL carp*”.

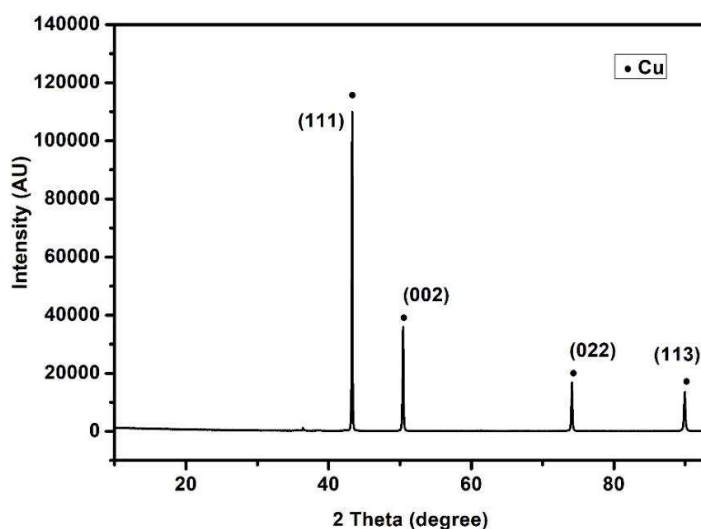


Figure 2.13- XRD analysis of copper powder

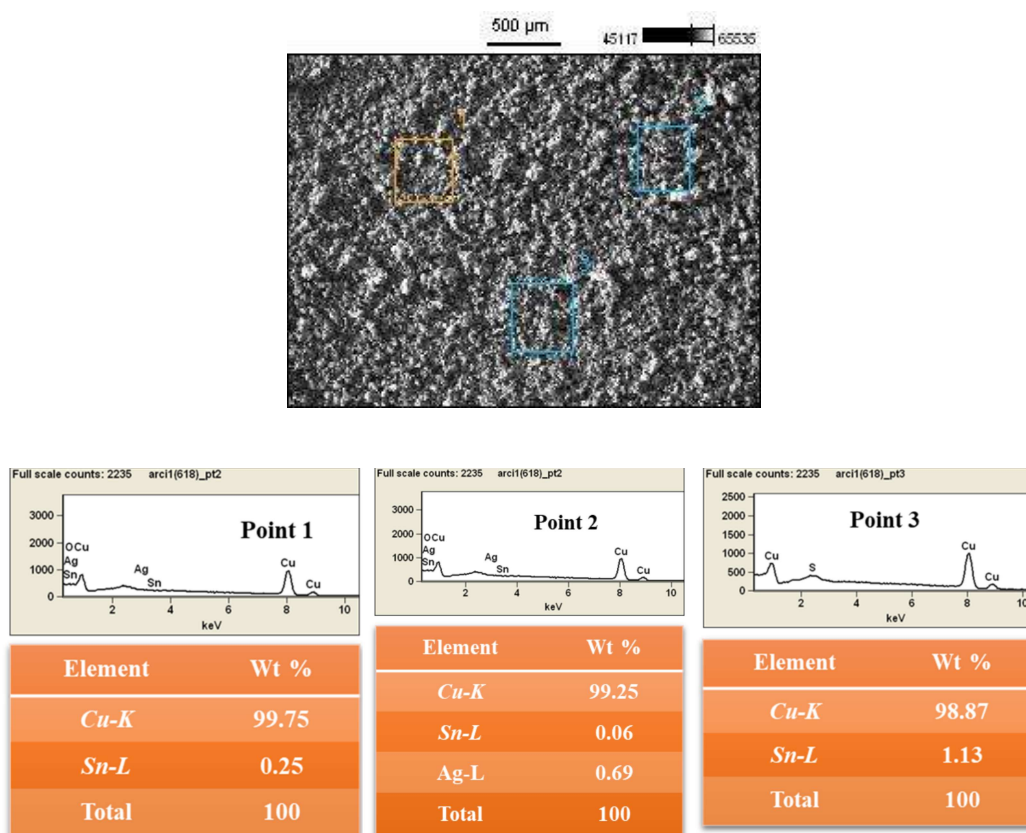


Figure 2.14- SEM-EDS of copper powder

The experimental studies were carried out by using a ceramic top type digital hot plate/magnetic stirrer with an attached PID temperature controlled and thermocouple (Accuracy  $\pm 1$  °C). During experiments, 100 mL of raffinate of gold solvent extraction stage solution was poured into a beaker and heated to desired temperature. Agitation was provided with magnetic stirring using a PTFE coated magnetic pellet. Once the fixed temperature was attained, copper powder was added to beaker slowly to yield good mixing without accumulation. Liquid samples were collected at regular intervals of time and sent for the chemical analysis to find out the concentration of elements. The solution is filtered after each experiment, and that residue is washed with distilled water, dried for 4 h at 80 °C in an oven, and characterized by SEM-EDS.

## 2.6.Characterization methods

### 2.6.1. Inductively coupled plasma-optical emission spectrophotometer (ICP-OES)

#### Principle:

Inductively Coupled Plasma-optical emission spectrophotometer is used to determine the metal ion concentration from an aqueous or organic solution by providing a suitable plasma. For plasma generation, argon gas and high-frequency electric current are initially applied to the working coil at the tip of the torch tube. The argon gas is ionized and plasma is generated with the help of an electromagnetic field by the high-frequency current. While plasma energy is given to analyze a liquid sample, the ions or atoms get excited. The excited atoms return to the low energy position, emission rays are released and the corresponding photon wavelength is measured. The element type is determined based on the position of the photon rays, and the concentration is determined based on the ray intensity. The emission is measured at a selected wavelength which is characteristic for each individual element. The emission measured is proportional to the

concentration of the metal ion. The metal content was determined by comparing this absorbance/ emission with the reference samples of a known set of standard solutions.

ICP-OES analysis was carried out using a Perkin Elmer Optima 8300 DC Inductively Coupled Plasma Optical Emission Spectrometer. Organic samples in 1-methoxy-2-propanol were taken up by a peristaltic pump at a rate of 2.0 mL min<sup>-1</sup> into a Gem Tip cross-flow nebulizer and a glass cyclonic spray chamber. Argon plasma conditions were 1500 W RF forward power and argon gas flows of 20, 1.4, and 0.45 L min<sup>-1</sup> for plasma, auxiliary, and nebulizer flow, respectively. ICP-OES calibration standards were obtained from VWR International or Sigma-Aldrich. Various metal ICP standards with 1, 5, 10, 25, 50 and 100 ppm of metals were used for the calibration.

### 2.6.2. Atomic absorption spectroscopy (AAS)

#### Principle:

Atomic absorption spectroscopy technique comprises the study of the absorption of radiant energy (usually visible and UV) by neutral atoms in the gaseous state. In this analysis, the metal ion being determined is reduced to its elemental state, vaporized, and subjected to the beam of radiation from the external light source. To create a flame, an oxidant gas (air/nitrous oxide) and a fuel gas (acetylene) is required. Usually, a hollow cathode lamp of the corresponding element is used to provide the light source at various wavelengths. To calibrate the AAS, the absorption of the solutions containing known amounts of elements is measured. The concentration of the elements can be determined based on the calibration curve which gives the relationship between absorbance and concentration as per beer-lamberts as shown in Eq. 2.1.

$$A = \lambda * b * c \quad (2.1)$$

A= Absorbance

$\lambda$  = Wavelength at which absorption is observed

b = path length

c= concentration

The analysis was carried out using an Elico Ltd Atomic AAS SL 168. Samples in distilled water were taken up by a PTFE (Teflon) capillary tube at a feed rate of  $5.0 \text{ mL min}^{-1}$  into a pneumatic nebulizer and a glass bead, High Density Poly Ethylene (HDPE) spray chamber. Air-acetylene flame conditions for the aqueous samples were:  $\text{C}_2\text{H}_2$  as a fuel with a pressure of 15 psi and a continuous, dry air as an oxidant with an input pressure of 50 psi. The flow rate of fuel and oxidant were 3 and  $2 \text{ L min}^{-1}$  respectively. AAS calibration standards were obtained from Sigma-Aldrich.

### 2.6.3. X-ray diffraction (XRD)

#### Principle:

X-ray powder diffraction is a primary analytical technique used for the phase identification, structure and composition analysis of crystalline material. This technique is based on the constructive interference of monochromatic x-rays and a crystalline sample. As x-rays have a wavelength in a range of interatomic spacing of a crystalline solid, the incident x-ray beam diffracts in specific directions as per Bragg's law [9]. The resulting diffraction pattern given by the intensities and positions of the diffraction effects provides information about structure identification.

The X-ray diffraction instrument was equipped with Co- $\text{K}\alpha$  radiation ( $\lambda=0.179 \text{ nm}$ ) (PANalytical EMPYREAN, 40kV-40mA) and Cu- $\text{K}\alpha$  radiation ( $\lambda=0.154 \text{ nm}$ ) (Rigaku miniflex-600, 40kV-15mA) were used for structural studies. XRD patterns were attained in the angular ( $2\theta$ ) range of  $10^\circ$  to  $100^\circ$  using  $0.02^\circ$  step size with a scan rate of  $10^\circ$  per

min. The ICDD (International Centre for Diffraction Data) PDF2 was used to analyze the presence of various phases in the diffraction pattern.

#### 2.6.4. UV-Visible spectrophotometer

##### Principle:

Absorption of visible or ultraviolet light with frequency ( $\nu$ ) and wavelength ( $\lambda$ ) results in the electronic transitions from lower to higher energy levels of the molecule. Uv-visible irradiation can excite an electron from a non-bonding (n), or a  $\pi$ -orbital to an antibonding  $\sigma$ -orbital ( $\sigma^*$ ) or an antibonding  $\pi$  orbital ( $\pi^*$ ). According to beer-lambert's principle, the absorbed incident radiation is directly proportional to the length of path it has travelled through the absorbing medium and the concentration of absorbing molecules in the solution. In addition, the fraction of incident radiation absorbed by a solute in a transparent solvent is independent of incident light intensity. Eq. 2.2. can express this law.

$$\text{Log } I_0/I = A = \epsilon cl \quad (2.2)$$

Where  $I_0$  = the intensity of incident light

$I$  = the intensity of transmitted light

$A$  = absorbance

$\epsilon$  = molar extinction coefficient or molar absorptivity

$c$  = concentration of solute, and

$l$  = cell path length

The measurements were performed on an 'Agilent Cary 60' spectrophotometer which consists of two light sources. A hydrogen or deuterium discharge tube scans the UV region in the range of 200-370 nm and a second source tungsten lamp covers the visible region in the range of 325-770 nm. All samples mentioned in the thesis were

appropriately diluted in ethanol and taken in a quartz cuvette of 1cm path length for UV-visible measurement.

### ***2.6.5. Scanning electron microscopy (SEM)***

#### Principle:

Scanning electron microscopy (SEM) is a high magnification microscope used to produce images of the sample at various magnifications with the help of a focused scanning electron beam. The interaction of the high-energy primary electron beam with the specimen produces two types of electrons. (i) Secondary electrons (SE) and (ii) Backscattered electrons. Secondary electrons possess low kinetic energy varying in the range of 0-50 eV, giving the sample topographic information. In contrast, backscattered electrons can produce images with a high degree of atomic number contrast. In addition, while SEM is joined with an EDX detector, the sample's chemical composition can also be produced by the production of x-rays.

Scanning Electron Microscopy (SEM) make *Zeiss Evo-18 Research 2045*, with Energy Dispersive X-ray Spectroscopy (EDS) attachment make *Oxford X-act INCA x-act* was used to determine the chemical composition of the samples mentioned in this thesis.

### ***2.6.6. Nuclear magnetic resonance Spectroscopy (NMR)***

#### Principle:

The nuclear magnetic spectroscopy (NMR) technique is usually used to determine the content, purity and molecular structure of the sample. The principle behind this technique is that many nuclei have spin and all nuclei are electrically charged. The energy transfer is possible between the base energy and a high energy level while an external magnetic field is applied. This energy transfer occurs at a particular radiofrequency wavelength and that energy is emitted while the spin returns to its base level. The signals that match

this energy transfer are measured in many ways and processed to produce an NMR spectrum for the nucleus concerned.

All NMR spectra were recorded at 300 K at the school of chemistry, the university of Edinburgh, Scotland, UK.  $^1\text{H}$ -NMR was performed on a Bruker AVA500 spectrometer at 500.12 MHz.